HHS Public Access

Author manuscript

DNA Repair (Amst). Author manuscript; available in PMC 2021 November 01.

Published in final edited form as:

DNA Repair (Amst). 2020 November ; 95: 102968. doi:10.1016/j.dnarep.2020.102968.

Yeast DNA polymerase η possesses two PIP-like motifs that bind PCNA and Rad6-Rad18 with different specificities

Brittany M. Ripley, **Devin T. Reusch**, **M. Todd Washington***

Department of Biochemistry, University of Iowa College of Medicine, Iowa City, IA 52242-1109

Abstract

In translesion synthesis (TLS), specialized DNA polymerases, such as polymerase (pol) η and Rev1, are recruited to stalled replication forks. These polymerases form a multi-protein complex with PCNA, Rad6-Rad18, and other specialized polymerases. Pol η interacts with PCNA and Rev1 via a PCNA-interacting protein (PIP) motif in its C-terminal unstructured region. Here we report the discovery of a second PIP-like motif in the C-terminal region of pol η, which we have designated as PIP2. We have designated the original PIP motif as PIP1. We show that the pol η PIP1 and PIP2 motifs bind PCNA with different affinities and kinetics. PIP1 binds with higher affinity than does PIP2, and PIP1 dissociates more slowly than does PIP2. In addition, we show that the interaction between pol η and Rad6-Rad18 is also mediated by the pol η PIP1 and PIP2 motifs. Again, we show that the affinity and kinetics by which these motifs bind Rad6-Rad18 is different. These findings are significant, because the multiple PIP-like motifs on pol η likely play quite different roles within the multi-protein complex formed at stalled replication forks. PIP1 likely plays a critical role in the recruiting pol η to this multi-protein complex. PIP2, by contrast, likely plays a critical role in maintaining the architecture and the dynamics of this multi-protein complex needed to maximize the efficiency and accuracy of TLS.

Keywords

DNA replication; DNA repair; mutagenesis; PCNA; translesion synthesis

1. Introduction

A variety of chemical agents as well as ionizing and ultraviolet (UV) radiation cause DNA damage (1). This damage poses a serious threat to genome stability and to cell viability, because it interferes with DNA replication. Since classical DNA polymerases cannot efficiently incorporate nucleotides opposite DNA lesions, replication forks stall upon

*To whom correspondence should be addressed: M. Todd Washington, Department of Biochemistry, 4-403 Bowen Science Building, University of Iowa, Iowa City, IA 52242-1109. Phone: 319-335-7518, Fax: 319-335-9570, todd-washington@uiowa.edu.

Author Statement

Brittany M. Ripley: Conceptualization, Methodology, Investigation, Validation, Funding acquisition, Writing- Original draft preparation. **Devin T. Reusch**: Investigation. **M. Todd Washington**: Conceptualization, Funding acquisition, Methodology, Writing-Reviewing and Editing.

encountering damage in the template strand. Translesion synthesis (TLS) is a pathway allowing cells to overcome such replication blocks (2–16). During this process, Rad6, a ubiquitin conjugating enzyme, and Rad18, a ubiquitin ligase, are recruited to stalled replication forks (16–28). The Rad6-Rad18 complex then catalyzes the mono-ubiquitylation of proliferating cell nuclear antigen (PCNA), the ring-shaped homotrimer that encircles DNA and acts as a sliding clamp (29). This is believed to recruit specialized TLS polymerases, such as DNA polymerase (pol) η and Rev1, to stalled replication forks (30). By contrast to classical polymerases, these specialized TLS polymerases can catalyze the efficient incorporation of nucleotides opposite DNA lesions.

Pol η is thought to be a first responder in TLS. It is rapidly recruited to stalled replication forks and is responsible for bypassing 8-oxoguanine lesions and UV radiation-induced thymine dimers in an error-free manner (31–35). Pol η interacts with a variety of other proteins including PCNA, Rev1, and Rad6-Rad18 (30,33,36–40). For example, yeast pol η interacts with both PCNA and Rev1 through a canonical PCNA-interacting protein (PIP) motif at its C-terminus (residues 621 to 628) (36,39). This motif has two adjacent, conserved hydrophobic/aromatic residues (F627 and F628) that can bind to a hydrophobic pocket on the front face of the PCNA ring or to a hydrophobic pocket on the C-terminal domain (CTD) of Rev1 (39,41–44). It is not known, however, what region of pol η is necessary for interactions with Rad6-Rad18.

During our studies of the interactions of pol η with PCNA, Rev1, and Rad6-Rad18, we unexpectedly discovered a second PIP motif in pol η. We designated this novel motif in pol η as PIP2, and we designated the original pol η PIP motif as PIP1. We found that the PIP1 and PIP2 motifs of pol η bind PCNA with different affinity and kinetics. PIP1 binds with higher affinity and with a significant long dwell time than does PIP2. Moreover, we found that both PIP1 and PIP2 mediate the interactions of pol η and Rad6-Rad18, with PIP1 binding with higher affinity than PIP2. These findings are significant, because the multiple PIP motifs on pol η likely play quite different roles within the multi-protein complex that carries out TLS. PIP1 likely plays a critical role in the recruiting pol η to this complex. PIP2, by contrast, likely plays a critical role in maintaining the architecture and the dynamics of this complex needed to maximize the efficiency and accuracy of TLS.

2. Materials and Methods

2.1. Genetic complementation studies

The wild type *RAD30* gene (which encodes pol η) under the control of its native promoter was cloned in yeast shuttle vector pKW108 to obtain pKW692. Site-directed mutagenesis was performed on the resulting plasmid to generate additional vectors, which contained mutant *rad30* genes encoding proteins with substitution in either PIP1 (S621A, F627A, and F628A) or PIP2 (S592A, L599A, and F600A). These plasmid constructs are described in Table S1. Plasmids were transformed into yeast strain Y25–5 *(rad5Δrad30Δ*), and the resulting strains were grown on synthetic media lacking leucine. Overnight cultures in selective media were diluted to 10^8, 10^7, and 10^6 cells/ml and plated on selective media. These plates were exposed to 0, 50, and 100 J/m^2 UV radiation and grown for 3 to 5 days in the dark. Yeast strain Y25–5 harboring plasmid pKW108 was used as a negative control.

2.2. Yeast two-hybrid assays

Yeast two-hybrid assays were conducted by inserting the wild-type *RAD30* gene or various mutant *rad30* genes into pGBDT7 to generate proteins containing pol η fused to the Gal4 DNA binding domain. The wild-type *POL30* gene (which encodes PCNA) and the wild-type *RAD18* gene were inserted into pGADT7 to generate proteins containing either PCNA or Rad18 fused to the Gal4 transcriptional activator. These plasmid constructs are described in Table S1. Plasmids were transformed into yeast strain AH109, which has a *HIS3* reporter gene, and transformed cells were plated on synthetic media lacking leucine and tryptophan. Overnight cultures in selective media were diluted to 10^8, 10^7, and 10^6 cells/ml and plated on either synthetic media lacking leucine and tryptophan; lacking histidine, leucine, and tryptophan; or lacking adenine, histidine, leucine, and tryptophan. Yeast strain AH109 harboring plasmids pGADT7 and pGBKT7 were used as negative controls.

2.3. Protein expression and purification

The yeast *RAD18* and *RAD6* genes were inserted into the multi-cloning site I and multi-cloning site II of pETDuet-1, respectively. The yeast *RAD6* gene was inserted into pET-11a. In both of these cases, the encoded Rad6 protein had a 6-His tag at its N-terminus. The yeast *POL30* gene was inserted into pET-11a. These plasmid constructs are described in Table S1. Rad6-Rad8 and Rad6 were over-expressed in BL21(DE3) by inducing cells at an OD_{600} of with 0.2 mM IPTG and 100 μM $ZnSo_4$ for 18 hours at 18° C. PCNA was over-expressed in BL21(DE3) by growing cells in Overnight Express media (Novagen) for 16 hours at 37° C. All proteins were purified at 4° C using a Ni-NTA Super Flow column (Qiagen), a DEAE Sepharose Fast Flow anion exchange column (GE Healthcare), and a HiLoad SuperDex 200 size-exclusion column (GE Healthcare). Proteins were concentrated using Amicon Ultra-4 10 K concentrator (Millipore). Protein aliquots were flash frozen with either 20 % glycerol for PCNA or 40 % glycerol for Rad6 and for Rad-Rad18. Proteins aliquots were stored at −80° C. Polyacrylamide gels of the purified proteins used in this study are shown in Fig. S1.

Peptides containing wild type and mutant forms of PIP1 and PIP2 of pol η were purchased from GenScript and possessed a biotin tag and an Ahx linker at their N-termini. Lyophilized peptides were resuspended in water, and the pH was adjusted to 7. Peptide aliquots were stored at −80° C. The sequences of the peptides are given in Table S2.

2.4. Biolayer interferometry

Biolayer interferometry (BLI) assays were carried out using an Octet RED96 system (ForteBio) at 28° C. BLI assays utilized a five-step protocol: equilibration (180 s), peptide ligand loading (20 to 60 s), baseline establishment (60 s), analyte association (various times), and analyte dissociation (various times). The analyte proteins (PCNA, Rad6-Rad18, or Rad6) were in BLI buffer (40 mM HEPES, pH 8, 150 mM NaCl, 0.5% bovine serum albumin, 0.002% Tween, and 5 mM 2-mercaptoethanol). The equilibration, baseline-establishment, and analyte-dissociation steps all used BLI buffer without analyte proteins. Prior to the experiment, the Streptavidin (SA) Biosensors (ForteBio) were soaked in BLI buffer for 10 min. Experiments were carried out with seven biosensors incubated with BLI buffer containing different concentrations of analyte. One biosensor was used as a reference and was incubated with BLI buffer without analyte. Control experiments were carried out

with sensors that were not loaded with peptide ligands to assess whether there was any non-specific analyte binding to the biosensors. The response units from non-specific binding was subtracted from the response units for the experiments that displayed non-specific binding. Data was processed with the ForteBio Data Analysis software and Prism (GraphPad).

3. Results

A combination of small-angle X-ray scattering (SAXS) and Langevin dynamics simulations showed that the C-terminal portion of pol η (residues 513–632) is intrinsically disordered (45). This portion of the protein is thought to act as a flexible tether linking the catalytic domain of pol η (residues 1 to 512) to various binding partners (Fig. 1A, Fig. S2). Scanning mutagenesis, in which ten amino acid residues at a time were changed to alanine residues, identified four regions within this C-terminal tether that are necessary for pol η function *in vivo* (45). Region 1 (residues 513 to 527) is immediately adjacent to the catalytic domain. Region 2 (residues 573 to 582) comprises part of the ubiquitin-binding, zinc-binding (UBZ) motif (residues 549 to 582), which likely binds the ubiquitin moiety on ubiquitin-modified PCNA (30). Region 3 (residues 593 to 607) has no known function. Region 4 (618 to 632) contains the canonical PIP motif (residues 621 to 628), which binds to PCNA and to the CTD or Rev1 (36,39). Visual examination of the region 3 revealed that it might contain a novel, non-canonical PIP motif (residues 593 to 600) (Fig. 1B). Here we show that this sequence motif is indeed a novel PIP motif, and we designate this motif as PIP2. We designate the established, canonical PIP motif (residues 621 to 628) as PIP1.

3.1. PIP1 and PIP2 are necessary for pol η function *in vivo*

Strains lacking a functional pol η protein are more sensitive to UV radiation than are strains producing wild-type pol η (46,47). In order to determine whether specific amino acid residues within PIP1 or PIP2 are necessary for pol η function *in vivo*, we carried out UV survival assays (Fig. 1C). As expected, strains producing a mutant pol η protein with substitutions in PIP1 (S621A, F627A, and F628A) were substantially more sensitive to UV radiation than strains producing wild-type pol η. Strains producing a mutant pol η with substitutions in PIP2 (S592A, L599A, and F600A) were more sensitive than strains producing wild-type pol η. Similarly, strains producing another mutant pol η with PIP2 substitutions (K589A, K596A, and R597A) were more sensitive than the wild-type strain. Overall, the strains with PIP2 substitutions in pol η were as sensitive as the strain with PIP1 substitutions in pol η. Moreover, strains producing a mutant pol η with both PIP1 and PIP2 substitutions (S621A, F627A, F628A, S592A, L599A, and F600A) were more sensitive than the wild-type strain. The strains with both PIP1 and PIP2 substitutions were approximately as sensitive as the strains with the PIP1 substitutions and the strains with the PIP2 substitutions.

3.2. PIP1 and PIP2 bind PCNA

To determine whether the PIP1 and PIP2 motifs of pol η are necessary for binding PCNA, we first utilized a yeast two-hybrid assay. Wild type pol η, a mutant pol η with substitutions in the hydrophobic/aromatic residues of PIP1 (S621A, F627A, and F628A), a mutant pol η with substitutions in the basic residues of PIP1 (K622A, R630A, K631A, and K632A), a

mutant pol η with substitutions in the hydrophobic/aromatic residues of PIP2 (S592A, L599A, and F600A), a mutant pol η with substitutions in the basic residues of PIP2 (K589A, K596A, and R597A), and a mutant pol η with substitutions in the hydrophobic/aromatic residues of both PIP1 and PIP2 were fused to the Gal4 DNA binding domain. PCNA was fused to the Gal4 transcriptional activator domain. A moderate-to-high affinity interaction between pol η and PCNA (with a K_d less than ~70 μM) results in growth on media without histidine, leucine, and tryptophan (-HLW). Under these conditions, we observed strong growth in all of the strains, except for those producing the mutant pol η protein with substitutions in the hydrophobic/aromatic residues of PIP1 and the mutant pol η protein with substitutions in the hydrophobic/aromatic residues of both PIP1 and PIP2 (Fig. 2). This shows that the wild type pol η protein, the mutant pol η protein with substitutions in the basic residues of PIP1, and the mutant pol η protein with substitutions in PIP2 bind to PCNA with higher affinity than does the mutant pol η protein with substitutions in the hydrophobic/aromatic residues of PIP1. A high affinity interaction between the pol η and PCNA results in growth on media without adenine, histidine, leucine, and tryptophan (-AHLW). Under these more stringent conditions, we observed growth of the strain producing the wild type pol η protein and the strain producing the mutant pol η protein with substitutions of the hydrophobic/aromatic residues in PIP2. We observed reduced growth of the strain producing the mutant pol η protein with substitutions of the basic residues in PIP2, and we observed no growth with any of the other strains. This shows that the wild type pol η protein and the mutant pol η protein with substitutions of the hydrophobic/aromatic residues in PIP2 binds to PCNA with higher affinity than do the other mutant proteins.

To examine quantitatively the thermodynamics and kinetics of the pol η PIP1 and PIP2 motifs binding to PCNA, we used biolayer interferometry (BLI). An N-terminally biotinylated peptide containing PIP1 was loaded onto the surface of streptavidin-coated BLI sensors. The sensors were dipped into wells contained various concentrations of PCNA to obtain association curves, and the sensors were dipped into wells containing buffer to obtain dissociation curves. By plotting the equilibrium response units as a function of PCNA concentration, we obtained a K_d for the PIP1-PCNA complex equal to 7.2 nM (Fig. 3A, B). Global fits of the dissociation phases yielded a first-order rate constant of dissociation (k_{off}) equal to 0.0054 s^{-1} corresponding to a dwell time for the PIP1-PCNA complex equal to 190 s.

We carried out similar experiments with the pol η PIP2 peptide (Fig. 3C, D). By plotting the equilibrium response units as a function of PCNA concentration, we obtained a K_d for the PIP2-PCNA complex equal to 13 μM. Global fits yielded a k_{off} equal to 0.30 s^{-1} corresponding to a dwell time of the PIP2-PCNA complex equal to 3.3 s.

To assess the contribution of the conserved serine and hydrophobic/aromatic residues in PIP1 and PIP2 to PCNA binding. We used peptides with either substitutions in PIP1 (S621A, F627A, F628A) or PIP2 (S592A, L499A, F600A). Using BLI, we observed no interactions between these peptides and PCNA (Fig. S3). This shows the requirement for these conserved residues in the PIP1 and PIP2 motifs for binding to PCNA.

3.3. PIP1 and PIP2 bind Rad6-Rad18

Human pol η binds to Rad6-Rad18, the ubiquitin conjugating enzyme and ubiquitin ligase that catalyze the mono-ubiquitylation of PCNA (33,38). It is unknown what regions of human pol η are required for this interaction. In order to determine whether yeast pol η binds Rad6-Rad18, we used a yeast two-hybrid assay. We observed strong growth on media lacking histidine, leucine, and tryptophan (-HLW) when wild type pol η was fused to the Gal4 DNA-binding domain and Rad18 was fused to the Gal4 transcriptional activator domain (Fig. 4A). This showed that wild type pol η interacts with Rad6-Rad18.

Yeast two-hybrid assays with a series of C-terminal truncation constructs of pol η suggested that the pol η PIP1 and PIP2 motifs may be necessary for interactions with Rad6-Rad18 (Fig. 4A). We observed a substantial reduction in the binding of Rad6-Rad18 for the pol η (1–623), pol η (1–606) and pol η (1–596) constructs. We observed a nearly complete loss of binding of Rad6-Rad18 for the pol η (1–586), pol η (1–561), and pol η (1–536) constructs. This indicates a region of pol η around residue 625 and another region around residue 595 are required for interactions with Rad6-Rad18. These regions are likely the PIP1 (residues 621 to 628) and PIP2 (residues 593 to 600) motifs, respectively.

To determine whether the pol η PIP1 and PIP2 motifs are indeed necessary for binding Rad6-Rad18, we carried out yeast two-hybrid assays with mutant forms of pol η with substitutions in PIP1 and PIP2 (Fig. 4B). A mutant form of pol η with the substituted serine and hydrophobic/aromatic residues in PIP1 (S621A, F627A, and F628A) did not interact with Rad6-Rad18. Surprisingly, a mutant form of pol η with the substituted serine and hydrophobic/aromatic residues in PIP2 (S592A, L599A, and F600A) was still able to interact with Rad6-Rad18), albeit with slightly lower affinity. Interestingly, a mutant form of pol η with the substituted basic residues in PIP2 (K589A, K596A, and R597A) did not interact with Rad6-Rad18. By contrast, a mutant form of pol η with the substituted basic residues in PIP1 (K622A, R630A, K631A, and K632A) was still able to interact with Rad6-Rad18. Thus, the conserved serine and hydrophobic/aromatic residues (but not the basic residues) of PIP1 mediate interactions with Rad6-Rad18, whereas the conserved basic residues (but not the serine and hydrophobic/aromatic residues) of PIP2 mediate interactions with Rad6-Rad18.

We carried out BLI experiments to examine quantitatively the thermodynamics and kinetics of the pol η PIP1 and PIP2 motifs binding to Rad6-Rad18. By plotting the equilibrium response units as a function of Rad6-Rad18 concentration, we obtained a K_d for the PIP1-Rad6-Rad18 complex equal to 1.2 μM (Fig. 5A, B). Global fits of the dissociation phases yielded a k_{off} equal to 0.00080 s^{-1} corresponding to a dwell time of the PIP1-Rad6-Rad18 complex equal to 1,300 s.

We carried out similar experiments with the pol η PIP2 peptide (Fig. 5C, D). By plotting the equilibrium response units as a function of Rad6-Rad18 concentration, we obtained a K_d for the complex equal to 3.7 μM. Global fits yielded a k_{off} equal to 0.13 s^{-1} corresponding to a dwell time of the PIP2-Rad6-Rad18 complex equal to 7.7 s.

To determine the role of the conserved serine and hydrophobic/aromatic residues in PIP1 and PIP2 to Rad6-Rad18 binding. We used peptides with either substitutions in PIP1 (S621A, F627A, F628A) or PIP2 (S592A, L499A, F600A). Using BLI, we observed significantly reduced binding of these peptides to Rad6-Rad18 (Fig. S4). This shows that the conserved serine and hydrophobic/aromatic residues in the PIP1 and PIP2 motifs are important for binding to Rad6-Rad18.

3.4. PIP1 bind Rad6 tightly, but PIP2 does not

Although Rad6-Rad18 forms a tight complex, Rad6 is stable by itself and can be purified in the absence of Rad18. Rad18, however, is not stable by itself and cannot be purified in the absence of Rad6. In order to understand better the structural basis of the interactions between the PIP1 and PIP2 motifs of pol η and Rad6-Rad18, we used BLI to determine whether these motifs directly bind Rad6 alone (Fig. 6). Surprisingly, we found that the pol η PIP1 binds Rad6 with nearly the same affinity as it binds Rad6-Rad18. By plotting the equilibrium response units as a function of Rad6 concentration, we obtained a K_d for the PIP1-Rad6 complex equal to 2.3 μM. Global fits yielded a k_{off} equal to 0.020 s^{-1} corresponding to a dwell time of the PIP1-Rad6 complex equal to 50 s. This interaction depended on the conserved serine and hydrophobic/aromatic residues in PIP1, because BLI experiments with these residues substituted resulted in a lack of binding (Fig. S5).

By contrast, we found that the pol η PIP2 binds Rad6 with significantly lower affinity than it binds Rad6-Rad18 (Fig. 6). By plotting the equilibrium response units as a function of Rad6 concentration, we obtained a K_d for the PIP2-Rad6 complex equal to 200 μM. Global fits yielded a k_{off} equal to 0.60 s^{-1}, corresponding to a dwell time of the PIP1-Rad6 complex equal to 1.7 s. Surprisingly, this interaction did not depend on the conserved serine and hydrophobic/aromatic residues in PIP2, because BLI experiments with these residues substituted resulted in only slightly reduced binding affinity with a K_d equal to 390 μM (Fig. S5). It is unclear why the binding affinity of the pol η PIP2 for Rad6 is weaker than its affinity for Rad6-Rad18. One possibility is that the presence of Rad18 stabilizes the interaction between the PIP2 and Rad6.

Rad6 binds the Rad6-binding domain (R6BD) of Rad18, which is located near the protein's C-terminus (residues 371–410) (16,38). Because Rad6 is a relatively small protein (172 amino acid residues), it is possible that the pol η PIP1 competes with the R6BD of Rad18 for binding Rad6. To determine whether this is the case, we carried out a BLI-based competition experiment (Fig. 7). An N-terminally biotinylated peptide containing the R6BD of Rad18 was loaded onto the surface of streptavidin-coated BLI sensors. The sensors were dipped into wells contained various concentrations of Rad6 alone or various concentrations of Rad6 with 20 μM of peptide containing the pol η PIP1. This concentration is nearly 10-fold greater than the K_d for the PIP1-Rad6 complex, so nearly all of the Rad6 should be bound to the pol η PIP1 under these conditions. By plotting the equilibrium response units as a function of Rad6 concentration, we obtained a K_d for the R6BD-Rad6 complex equal to 2.5 μM in the absence of the pol η PIP1 and a K_d for the complex equal to 2.8 μM in the presence of the pol η PIP1. This shows that the pol η PIP1 does not compete with the R6BD of Rad18 for binding Rad6.

Finally, the discovery that Rad6 binds the pol η PIP1 with significantly higher affinity than it binds the pol η PIP2 raised the question of whether Rad6 can bind PIP-like motifs from other proteins. We carried out BLI experiments to examine the ability of Rad6 to bind the PIP-like motif of Pol32 (a non-catalytic subunit of both pol δ and pol ς), Msh6 (a mismatch repair protein), and Rad5 (a replication fork-remodeling helicase). We did not observe Rad6 binding either the PIP-like of Msh6 or the PIP-like motif of Rad5 (Fig. S6). However, we obtained a K_d for the complex between Rad6 and the PIP-like motif of Pol32 equal to 0.6 μM (Fig. S6), which is very similar to the affinity of the pol η PIP1 binding Rad6.

4. Discussion

PIP motifs have typically been thought of as strictly PCNA-interacting motifs (48–51). The conserved hydrophobic/aromatic residues of these motifs bind in a hydrophobic pocket on the front face of the PCNA ring (41,42). Recently, however, a number of findings have shown that PIP motifs are more versatile than previously believed (44). For example, the conserved hydrophobic/aromatic residues of PIP-like motifs in human TLS pol η, pol ι, and pol κ as well as in yeast fork-remodeling helicase Rad5 bind in a hydrophobic pocket on the CTD of TLS polymerases Rev1 (43,52–54). These PIP-like motifs are sometimes referred to as Rev1-interacting region (RIR) motifs. Similarly, the conserved hydrophobic/aromatic residues of PIP-like motifs in yeast exonuclease Exo1 and yeast DNA glycosylase Ntg2 bind in a hydrophobic pocket on mismatch repair protein Mlh1 (55). These PIP-like motifs are sometimes referred to as Mlh1-interacting protein (MIP) motifs. Likewise, the conserved hydrophobic/aromatic residues of a PIP-like motif in human TLS pol η bind in a hydrophobic pocket on the non-catalytic POLD2 subunit of human classical pol δ (56). This PIP-like motif is sometimes referred to as a F1 motif.

In the case of yeast pol η, the conserved hydrophobic/aromatic residues of the PIP1 motif have been shown to bind to PCNA and to the CTD of Rev1 in a mutually exclusive manner (39,40). These interactions have led to the notion that the multi-protein complex formed by pol η, PCNA, and Rev1 can exist in only two possible architectures: PCNA tool belts and Rev1 bridges (15,40). In a PCNA tool belt, pol η directly interacts with one subunit of PCNA via the pol η PIP1 motif, while Rev1 directly interacts with a different subunit of PCNA via the Rev1 BRCT domain. In a PCNA tool belt, pol η and Rev1 do not directly interact with each other. By contrast, in a Rev1 bridge, pol η directly interacts with Rev1 via the pol η PIP1 motif, while PCNA directly interacts with Rev1 via the Rev1 BRCT domain. In a Rev1 bridge, pol η and PCNA do not directly interact with each other. Single-molecule total internal reflection fluorescence (TIRF) microscopy-based experiments have shown both PCNA tool belts and Rev1 bridges form among these three proteins at approximately equal frequencies (40).

Here we have shown that the PIP1 motif of yeast pol η also binds to the ubiquitin-conjugating enzyme Rad6, which is required for TLS. This again highlights the remarkable versatility of this short protein-protein interaction motif. This PIP1-mediated interaction between pol η and Rad6-Rad18 is biological significant. For example, one of the major outstanding questions in the field is the role of PCNA ubiquitylation in promoting TLS. It is widely believed that because specialized TLS polymerases typically have tandem PIP motifs

and ubiquitin-binding motifs, the ubiquitylation of PCNA acts as a signal to recruit these polymerases to sites of stalled replication. Two observations in the literature, however, are difficult to reconcile with this notion. First, the interaction between pol η and Rad6-Rad18 promotes the localization of pol η to DNA damage foci *in vivo* (33–35). Second, the pol η and Rad6-Rad18 interaction actually promotes the transfer of ubiquitin from Rad6 to PCNA, suggesting that pol η is already in the complex when the ubiquitin transfer reaction occurs (35). Taken together, these observations support a model in which pol η can be recruited to stalled replication forks by riding piggyback on Rad6-Rad18 as it is directed toward the PCNA at these forks (16). Moreover, the discovery that the PIP1 motif of pol η interacts with Rad6 may provide a structural basis for the recruitment of pol η to stalled replication forks.

In the present study, we report the discovery of a second PIP-like motif, which we have designated PIP2, within the intrinsically disordered C-terminal region of yeast pol η. This motif binds to both PCNA and to Rad6-Rad18, but it does so with substantially lower affinity than does PIP1. Examining the kinetics of PIP1 and PIP2 binding to and releasing from PCNA and Rad6-Rad18 indicate that PIP2 binds to and releases from its target proteins faster than does PIP1. This makes the interaction between PIP2 and its target proteins less kinetically stable than the interaction between PIP1 and its target proteins. For example, the dwell time of the PIP1-PCNA complex is 190 s, and the dwell time of the PIP2-PCNA complex is 3.3 s. Similarly, the dwell time of the PIP1-Rad6-Rad18 complex is 1,300 s, and the dwell time of the PIP2-Rad6-Rad18 complex is 7.7 s. This large difference in the thermodynamics and kinetics of PIP1 and PIP2 interactions with their target proteins suggests that these motifs play quite different roles within the multi-protein complexes that they form. We suggest that PIP1 plays the predominant role in mediating the interaction between pol η and PCNA, whereas PIP2 plays a role in maintaining the architecture of multi-protein complexes formed by pol η and PCNA.

One surprising result from prior studies of the multi-protein complexes formed among pol η, Rev1, and PCNA is that the architecture of these complexes can change without any proteins dissociating from the complex (40). For example, about 20 % of the complexes that initially formed as PCNA tool belts changed architectures to Rev1 bridges without any proteins dissociating. Similarly, about 20 % of the complexes that initially formed as Rev1 bridges changed architectures to PCNA tool belts without any proteins dissociating. It has been proposed that such architectural changes in the multi-protein complexes containing TLS polymerases facilitates the sampling of the template DNA lesion by multiple TLS polymerases to find the one that can catalyze nucleotide incorporation most efficiently (15). This so-called kinetic selection model, which maximizes both the efficiency and accuracy of TLS, is likely driven in part by these architectural changes.

The presence of PIP2 in the C-terminal region of pol η may provide a structural basis for how the architecture of these multi-protein complexes can change without any proteins dissociating (Fig. 8A). Consider a switch from a PCNA tool belt to a Rev1 bridge. In the PCNA tool belt, the PIP1 of pol η would be bound to the hydrophobic pocket on one subunit of PCNA. While the Rev1 CTD would be available to bind the pol η PIP1, directly releasing the PIP1 motif from PCNA would lead to the dissociating of pol η. If, however, the PIP2,

with its lower affinity and shorter half-life of binding, were to bind to a hydrophobic pocket on a different subunit of PCNA, it could transiently prevent pol η from dissociating from PCNA while it transfers its PIP1 motif from PCNA to the Rev1 CTD. Likewise, consider a switch from a Rev1 bridge to a PCNA tool belt. In the Rev1 bridge, the pol η PIP1 would be bound to the CTD of Rev1. While PCNA is available to bind the pol η PIP1, directly releasing the PIP1 motif from Rev1 would lead to the dissociating of pol η. If, however, the PIP2 were to bind to a hydrophobic pocket on one subunit of PCNA, it again could transiently prevent pol η from dissociating from PCNA while it transferred its PIP1 motif from Rev1 to a different subunit of PCNA.

Two conditions would need to be met for such a mechanism to occur. First, the pol η PIP1 motif and PIP2 motif would have to be capable of binding to two subunits of a PCNA trimer at the same time. Our structural modeling shows that the PIP1 and PIP2 motifs are far enough apart in the C-terminal region of pol η that both motifs could simultaneously bind PCNA (Fig. 8B). Second, the pol η PIP2 motif must bind to one of the hydrophobic pockets on the front of PCNA with high occupancy. Despite its relatively modest affinity for PCNA, we expect this to be the case. This is because the interaction between pol η and PCNA is mediated by the high affinity interaction with PIP1. This would greatly increase the local concentration of PIP2 ensuring that it will be bound to another PCNA subunit with a high frequency. Although future structural and single-molecule studies will be necessary to understand the details of this process, the discovery of the pol η PIP2 motif substantially expands our understanding of the dynamic multi-protein complexes that carry out TLS.

Supplementary Material

Refer to Web version on PubMed Central for supplementary material.

Acknowledgments

This research was funded by the National Institute of General Medical Sciences, grant number GM081433. The content is solely the responsibility of the authors and does not necessarily reflect the official views of the National Institute of General Medical Sciences or the National Institutes of Health. We thank Christine Kondratick, Justin Ling, Melissa Gildenberg, Kyle Powers, and Elizabeth Boehm for discussions.

Abbreviations

The abbreviations used are:

CTD	C-terminal domain
PCNA	proliferating cell nuclear antigen
PIP	PCNA-interacting protein
pol	polymerase
SAXS	small-angle X-ray scattering
TLS	translesion synthesis
UBZ	ubiquitin-binding, zinc-binding

UV	ultraviolet

References

1. Friedberg ECW, G. C.; Siede W; Wood RD; Schultz RA; Ellenberger T. (2006) DNA Repair and Mutagenesis. 2nd Edition ed. American Society of Microbiology Press.
2. Friedberg EC, Wagner R and Radman M. (2002) Specialized DNA polymerases, cellular survival, and the genesis of mutations. Science, 296, 1627–1630. [PubMed: 12040171]
3. Lawrence CW (2002) Cellular roles of DNA polymerase zeta and Rev1 protein. DNA repair, 1, 425–435. [PubMed: 12509231]
4. Prakash S and Prakash L. (2002) Translesion DNA synthesis in eukaryotes: a one- or two-polymerase affair. Genes & development, 16, 1872–1883. [PubMed: 12154119]
5. Lehmann AR (2003) Replication of damaged DNA. Cell cycle, 2, 300–302. [PubMed: 12851478]
6. Prakash S, Johnson RE and Prakash L. (2005) Eukaryotic translesion synthesis DNA polymerases: specificity of structure and function. Annual review of biochemistry, 74, 317–353.
7. Lehmann AR (2005) Replication of damaged DNA by translesion synthesis in human cells. FEBS letters, 579, 873–876. [PubMed: 15680966]
8. Lehmann AR, Niimi A, Ogi T, Brown S, Sabbioneda S, Wing JF, Kannouche PL and Green CM (2007) Translesion synthesis: Y-family polymerases and the polymerase switch. DNA repair, 6, 891–899. [PubMed: 17363342]
9. Waters LS, Minesinger BK, Wiltrout ME, D'Souza S, Woodruff RV and Walker GC (2009) Eukaryotic translesion polymerases and their roles and regulation in DNA damage tolerance. Microbiology and molecular biology reviews : MMBR, 73, 134–154. [PubMed: 19258535]
10. Washington MT, Carlson KD, Freudenthal BD and Pryor JM (2010) Variations on a theme: eukaryotic Y-family DNA polymerases. Biochimica et biophysica acta, 1804, 1113–1123. [PubMed: 19616647]
11. Sale JE, Lehmann AR and Woodgate R. (2012) Y-family DNA polymerases and their role in tolerance of cellular DNA damage. Nature reviews. Molecular cell biology, 13, 141–152. [PubMed: 22358330]
12. Boiteux S and Jinks-Robertson S. (2013) DNA repair mechanisms and the bypass of DNA damage in Saccharomyces cerevisiae. Genetics, 193, 1025–1064. [PubMed: 23547164]
13. Pryor JM, Dieckman LM, Boehm EM and Washington MT (2014) Eukaryotic Y-Family Polymerases: A Biochemical and Structural Perspective. Nucleic Acids Mol Bi, 30, 85–108.
14. Marians KJ (2018) Lesion Bypass and the Reactivation of Stalled Replication Forks. Annual review of biochemistry.
15. Powers KT and Washington MT (2018) Eukaryotic translesion synthesis: Choosing the right tool for the job. DNA repair, 71, 127–134. [PubMed: 30174299]
16. Ripley BM, Gildenberg MS and Washington MT (2020) Control of DNA Damage Bypass by Ubiquitylation of PCNA. Genes, 11.
17. Hoege C, Pfander B, Moldovan GL, Pyrowolakis G and Jentsch S. (2002) RAD6-dependent DNA repair is linked to modification of PCNA by ubiquitin and SUMO. Nature, 419, 135–141. [PubMed: 12226657]
18. Stelter P and Ulrich HD (2003) Control of spontaneous and damage-induced mutagenesis by SUMO and ubiquitin conjugation. Nature, 425, 188–191. [PubMed: 12968183]
19. Moldovan GL, Pfander B and Jentsch S. (2007) PCNA, the maestro of the replication fork. Cell, 129, 665–679. [PubMed: 17512402]
20. Bergink S and Jentsch S. (2009) Principles of ubiquitin and SUMO modifications in DNA repair. Nature, 458, 461–467. [PubMed: 19325626]
21. Shaheen M, Shanmugam I and Hromas R. (2010) The Role of PCNA Posttranslational Modifications in Translesion Synthesis. J Nucleic Acids, 2010.
22. Ulrich HD and Walden H. (2010) Ubiquitin signalling in DNA replication and repair. Nature reviews. Molecular cell biology, 11, 479–489. [PubMed: 20551964]

23. Dieckman LM, Freudenthal BD and Washington MT (2012) PCNA structure and function: insights from structures of PCNA complexes and post-translationally modified PCNA. Sub-cellular biochemistry, 62, 281–299. [PubMed: 22918591]
24. Ulrich HD and Takahashi T. (2013) Readers of PCNA modifications. Chromosoma, 122, 259–274. [PubMed: 23580141]
25. Boehm EM, Gildenberg MS and Washington MT (2016) The Many Roles of PCNA in Eukaryotic DNA Replication. The Enzymes, 39, 231–254. [PubMed: 27241932]
26. Cipolla L, Maffia A, Bertoletti F and Sabbioneda S. (2016) The Regulation of DNA Damage Tolerance by Ubiquitin and Ubiquitin-Like Modifiers. Front Genet, 7, 105. [PubMed: 27379156]
27. Choe KN and Moldovan GL (2017) Forging Ahead through Darkness: PCNA, Still the Principal Conductor at the Replication Fork. Molecular cell, 65, 380–392. [PubMed: 28157503]
28. Kanao R and Masutani C. (2017) Regulation of DNA damage tolerance in mammalian cells by post-translational modifications of PCNA. Mutation research, 803–805, 82–88.
29. Krishna TS, Kong XP, Gary S, Burgers PM and Kuriyan J. (1994) Crystal structure of the eukaryotic DNA polymerase processivity factor PCNA. Cell, 79, 1233–1243. [PubMed: 8001157]
30. Bienko M, Green CM, Crosetto N, Rudolf F, Zapart G, Coull B, Kannouche P, Wider G, Peter M, Lehmann AR et al. (2005) Ubiquitin-binding domains in Y-family polymerases regulate translesion synthesis. Science, 310, 1821–1824. [PubMed: 16357261]
31. Johnson RE, Prakash S and Prakash L. (1999) Efficient bypass of a thymine-thymine dimer by yeast DNA polymerase, Poleta. Science, 283, 1001–1004. [PubMed: 9974380]
32. Haracska L, Yu SL, Johnson RE, Prakash L and Prakash S. (2000) Efficient and accurate replication in the presence of 7,8-dihydro-8-oxoguanine by DNA polymerase eta. Nature genetics, 25, 458–461. [PubMed: 10932195]
33. Watanabe K, Tateishi S, Kawasuji M, Tsurimoto T, Inoue H and Yamaizumi M. (2004) Rad18 guides poleta to replication stalling sites through physical interaction and PCNA monoubiquitination. The EMBO journal, 23, 3886–3896. [PubMed: 15359278]
34. Despras E, Delrieu N, Garandeau C, Ahmed-Seghir S and Kannouche PL (2012) Regulation of the specialized DNA polymerase eta: revisiting the biological relevance of its PCNA- and ubiquitin-binding motifs. Environ Mol Mutagen, 53, 752–765. [PubMed: 23076824]
35. Durando M, Tateishi S and Vaziri C. (2013) A non-catalytic role of DNA polymerase eta in recruiting Rad18 and promoting PCNA monoubiquitination at stalled replication forks. Nucleic acids research, 41, 3079–3093. [PubMed: 23345618]
36. Haracska L, Kondratick CM, Unk I, Prakash S and Prakash L. (2001) Interaction with PCNA is essential for yeast DNA polymerase eta function. Molecular cell, 8, 407–415. [PubMed: 11545742]
37. Haracska L, Johnson RE, Unk I, Phillips B, Hurwitz J, Prakash L and Prakash S. (2001) Physical and functional interactions of human DNA polymerase eta with PCNA. Molecular and cellular biology, 21, 7199–7206. [PubMed: 11585903]
38. Notenboom V, Hibbert RG, van Rossum-Fikkert SE, Olsen JV, Mann M and Sixma TK (2007) Functional characterization of Rad18 domains for Rad6, ubiquitin, DNA binding and PCNA modification. Nucleic acids research, 35, 5819–5830. [PubMed: 17720710]
39. Boehm EM, Powers KT, Kondratick CM, Spies M, Houtman JC and Washington MT (2016) The Proliferating Cell Nuclear Antigen (PCNA)-interacting Protein (PIP) Motif of DNA Polymerase eta Mediates Its Interaction with the C-terminal Domain of Rev1. The Journal of biological chemistry, 291, 8735–8744. [PubMed: 26903512]
40. Boehm EM, Spies M and Washington MT (2016) PCNA tool belts and polymerase bridges form during translesion synthesis. Nucleic acids research, 44, 8250–8260. [PubMed: 27325737]
41. Gulbis JM, Kelman Z, Hurwitz J, O'Donnell M and Kuriyan J. (1996) Structure of the C-terminal region of p21(WAF1/CIP1) complexed with human PCNA. Cell, 87, 297–306. [PubMed: 8861913]
42. Hishiki A, Hashimoto H, Hanafusa T, Kamei K, Ohashi E, Shimizu T, Ohmori H and Sato M. (2009) Structural basis for novel interactions between human translesion synthesis polymerases and proliferating cell nuclear antigen. The Journal of biological chemistry, 284, 10552–10560. [PubMed: 19208623]

43. Pozhidaeva A, Pustovalova Y, D'Souza S, Bezsonova I, Walker GC and Korzhnev DM (2012) NMR structure and dynamics of the C-terminal domain from human Rev1 and its complex with Rev1 interacting region of DNA polymerase eta. Biochemistry, 51, 5506–5520. [PubMed: 22691049]
44. Boehm EM and Washington MT (2016) R.I.P. to the PIP: PCNA-binding motif no longer considered specific: PIP motifs and other related sequences are not distinct entities and can bind multiple proteins involved in genome maintenance. BioEssays : news and reviews in molecular, cellular and developmental biology, 38, 1117–1122.
45. Powers KT, Elcock AH and Washington MT (2018) The C-terminal region of translesion synthesis DNA polymerase eta is partially unstructured and has high conformational flexibility. Nucleic acids research, 46, 2107–2120. [PubMed: 29385534]
46. McDonald JP, Levine AS and Woodgate R. (1997) The Saccharomyces cerevisiae RAD30 gene, a homologue of Escherichia coli dinB and umuC, is DNA damage inducible and functions in a novel error-free postreplication repair mechanism. Genetics, 147, 1557–1568. [PubMed: 9409821]
47. Johnson RE, Prakash S and Prakash L. (1999) Requirement of DNA polymerase activity of yeast Rad30 protein for its biological function. The Journal of biological chemistry, 274, 15975–15977. [PubMed: 10347143]
48. Tsurimoto T. (1999) PCNA binding proteins. Frontiers in bioscience : a journal and virtual library, 4, D849–858. [PubMed: 10577396]
49. Hingorani MM and O'Donnell M. (2000) Sliding clamps: a (tail)ored fit. Current biology : CB, 10, R25–29. [PubMed: 10660290]
50. Warbrick E. (2000) The puzzle of PCNA's many partners. BioEssays : news and reviews in molecular, cellular and developmental biology, 22, 997–1006.
51. Maga G and Hubscher U. (2003) Proliferating cell nuclear antigen (PCNA): a dancer with many partners. Journal of cell science, 116, 3051–3060. [PubMed: 12829735]
52. Wojtaszek J, Lee CJ, D'Souza S, Minesinger B, Kim H, D'Andrea AD, Walker GC and Zhou P. (2012) Structural basis of Rev1-mediated assembly of a quaternary vertebrate translesion polymerase complex consisting of Rev1, heterodimeric polymerase (Pol) zeta, and Pol kappa. The Journal of biological chemistry, 287, 33836–33846. [PubMed: 22859295]
53. Wojtaszek J, Liu J, D'Souza S, Wang S, Xue Y, Walker GC and Zhou P. (2012) Multifaceted recognition of vertebrate Rev1 by translesion polymerases zeta and kappa. The Journal of biological chemistry, 287, 26400–26408. [PubMed: 22700975]
54. Xu X, Lin A, Zhou C, Blackwell SR, Zhang Y, Wang Z, Feng Q, Guan R, Hanna MD, Chen Z et al. (2016) Involvement of budding yeast Rad5 in translesion DNA synthesis through physical interaction with Rev1. Nucleic acids research.
55. Gueneau E, Dherin C, Legrand P, Tellier-Lebegue C, Gilquin B, Bonnesoeur P, Londino F, Quemener C, Le Du MH, Marquez JA et al. (2013) Structure of the MutLalpha C-terminal domain reveals how Mlh1 contributes to Pms1 endonuclease site. Nature structural & molecular biology, 20, 461–468.
56. Baldeck N, Janel-Bintz R, Wagner J, Tissier A, Fuchs RP, Burkovics P, Haracska L, Despras E, Bichara M, Chatton B et al. (2015) FF483–484 motif of human Poleta mediates its interaction with the POLD2 subunit of Poldelta and contributes to DNA damage tolerance. Nucleic acids research, 43, 2116–2125. [PubMed: 25662213]

Highlights

- Yeast pol η possesses a second PIP motif, which we have named PIP2
- The PIP motifs of pol η bind PCNA with different affinity and kinetics
- The PIP motifs of pol η bind Rad6-Rad18 with different affinity and kinetics
- PIP1 likely recruits pol η to translesion synthesis complexes
- PIP2 likely facilitates the dynamics of translesion synthesis complexes

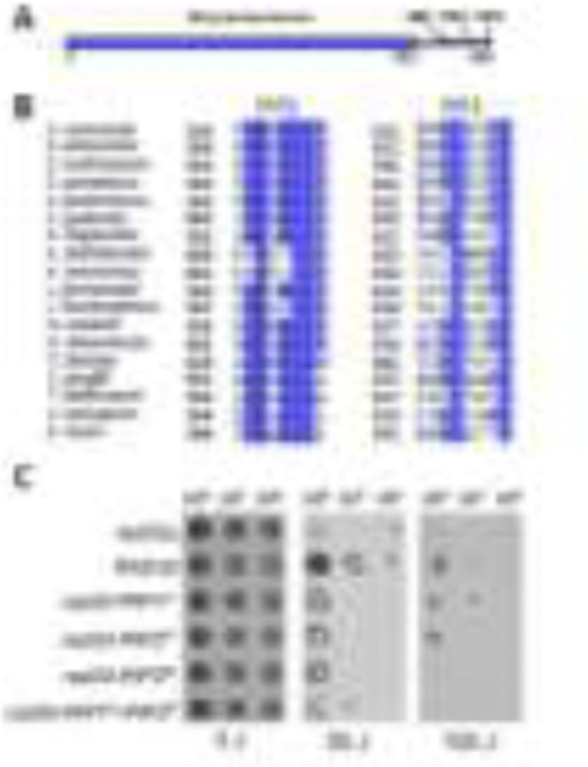

Figure 1. The PIP1 and PIP2 motifs of pol η are necessary for function *in vivo*.

(**A**) A diagram of full-length pol η with the polymerase domain shown as a thick blue rectangle and the unstructured C-terminal region shown as a thin grey rectangle. The locations of the PIP1, PIP2, and UBZ motifs in the C-terminal region are shown in blue. (**B**) A sequence alignment of PIP1 and PIP2 from 18 yeast species is shown. Conserved residues are highlighted in blue. (**C**) The survival of yeast strains expressing no gene for the pol η protein (*rad30Δ*), the gene for the wild type pol η protein (*RAD30*), the gene for the mutant pol η protein with substitutions of the hydrophobic/aromatic residues in PIP1 (*rad30-PIP1*^{H}), the gene for the mutant pol η protein with substitutions of the hydrophobic/aromatic residues in PIP2 (*rad30-PIP2*^{H}), the gene for the mutant pol η protein with substitutions of the basic residues in PIP2 (*rad30-PIP2*^{B}), and the gene for the mutant pol η protein with substitutions of the hydrophobic/aromatic residues in both PIP1 and PIP2 are shown at various exposures to UV radiation.

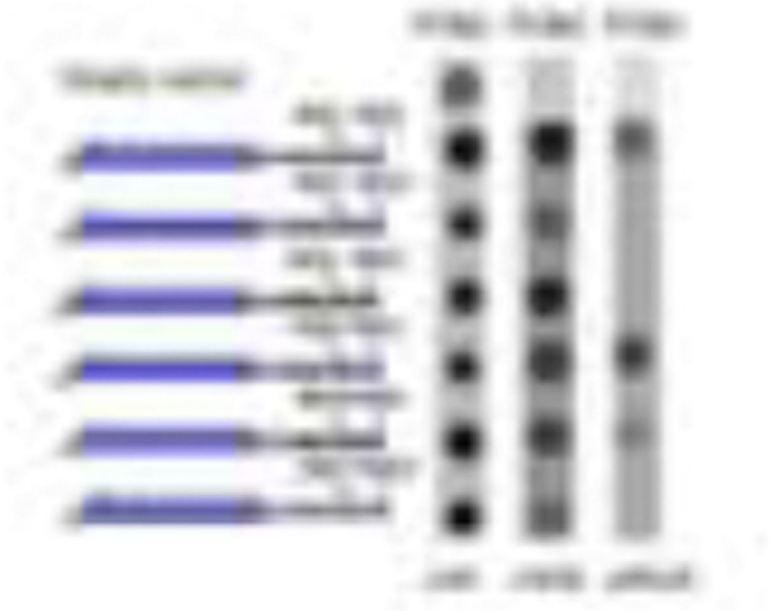

Figure 2. The PIP1 and PIP2 motifs of pol η are necessary for interacting with PCNA.

Yeast two-hybrid studies were carried out to examine the interactions of the wild type pol η protein, the mutant pol η protein with substitutions of the hydrophobic/aromatic residues in PIP1 ($PIP1^{H}$), the mutant pol η protein with substitutions of the basic residues in PIP1 ($PIP1^{B}$), the mutant pol η protein with substitutions of the hydrophobic/aromatic residues in PIP2 ($PIP2^{H}$) with PCNA, the mutant pol η protein with substitutions of the basic residues in PIP2 ($PIP2^{B}$), and the mutant pol η protein with substitutions of the hydrophobic/aromatic residues in both PIP1 and PIP2 ($PIP1^{H}$ $PIP2^{H}$). Growth on media lacking leucine and tryptophan (-LW) indicates the presence of both two-hybrid plasmids. Growth on media lacking histidine, leucine, and tryptophan (-HLW) indicates the presence of an interaction between the two proteins. Growth on media lacking adenine, histidine, leucine, and tryptophan (-AHLW) indicates the presence of a high-affinity interaction between the two proteins.

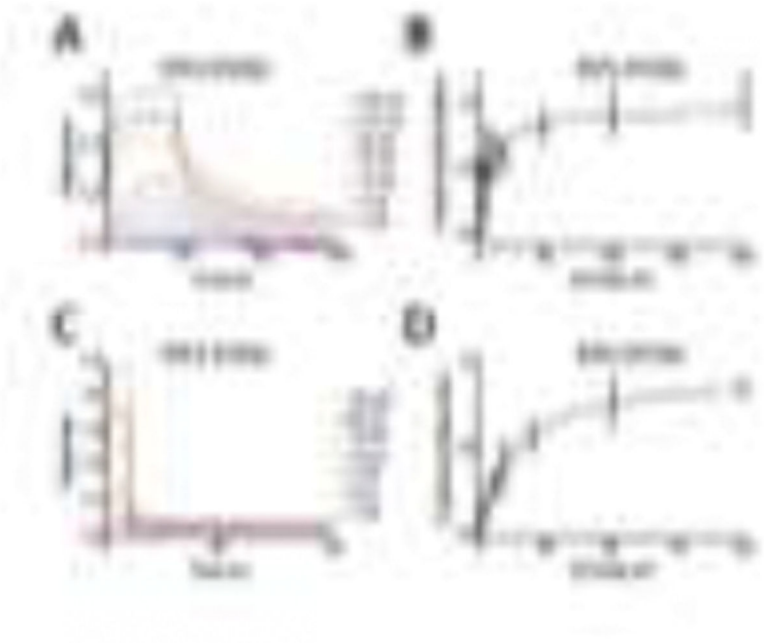

Figure 3. The PIP1 and PIP2 motifs of pol η bind PCNA with different affinities.

(**A**) The response units from BLI were graphed as a function of time for a fixed concentration of the PIP1 of pol η and various concentrations of PCNA (2 to 200 nM). The association phase spanned 0 to 100 s, and the dissociation phase spanned 100 to 300 s. (**B**) The equilibrium response units for each concentration of PCNA were expressed as fractional saturation and graphed as a function of PCNA concentration. The best fit of the data to the Adair equation yielded a K_d equal to 7.2 ± 2.4 nM. (**C**) The response units from BLI were graphed as a function of time for a fixed concentration of the PIP2 of pol η and various concentrations of PCNA (1 to 100 μM). The association phase spanned 0 to 10 s, and the dissociation phase spanned 10 to 100 s. (**D**) The equilibrium response units for each concentration of PCNA were expressed as fractional saturation and graphed as a function of PCNA concentration. The best fit of the data to the Adair equation yielded a K_d equal to 12 ± 2 μM.

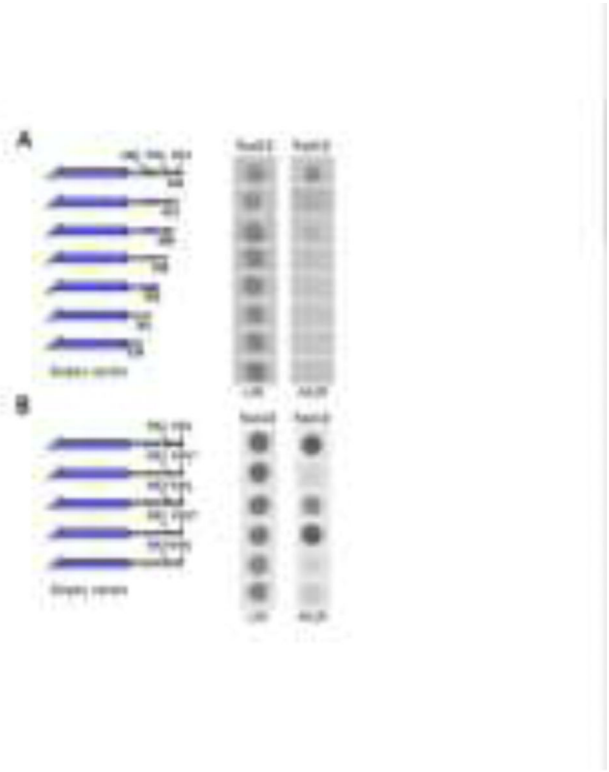

Figure 4. The PIP1 and PIP2 motifs of pol η are necessary for interacting with Rad6-Rad18.

(**A**) Yeast two-hybrid studies were carried out to examine the interactions of the full-length pol η (1–632) and various truncated forms of pol η (1–623, 1–606, 1–596, 1–586, 1–561, and 1–536) with the Rad18 subunit of Rad6-Rad18. Growth on media lacking leucine and tryptophan (-LW) indicates the presence of both two-hybrid plasmids. Growth on media lacking histidine, leucine, and tryptophan (-HLW) indicates the presence of an interaction between the two proteins. (**B**) Yeast two-hybrid studies were carried out to examine the interactions of the wild type pol η protein, the mutant pol η protein with substitutions of the hydrophobic/aromatic residues in PIP1 ($PIP1^{H}$), the mutant pol η protein with substitutions of the hydrophobic/aromatic residues in PIP2 ($PIP2^{H}$), the mutant pol η protein with substitutions of the basic residues in PIP1 ($PIP1^{B}$), and the mutant pol η protein with substitutions of the basic residues in PIP2 ($PIP2^{B}$) with the Rad18 subunit of Rad6-Rad18. Growth on media lacking leucine and tryptophan (-LW) indicates the presence of both two-hybrid plasmids. Growth on media lacking histidine, leucine, and tryptophan (-HLW) indicates the presence of an interaction between the two proteins.

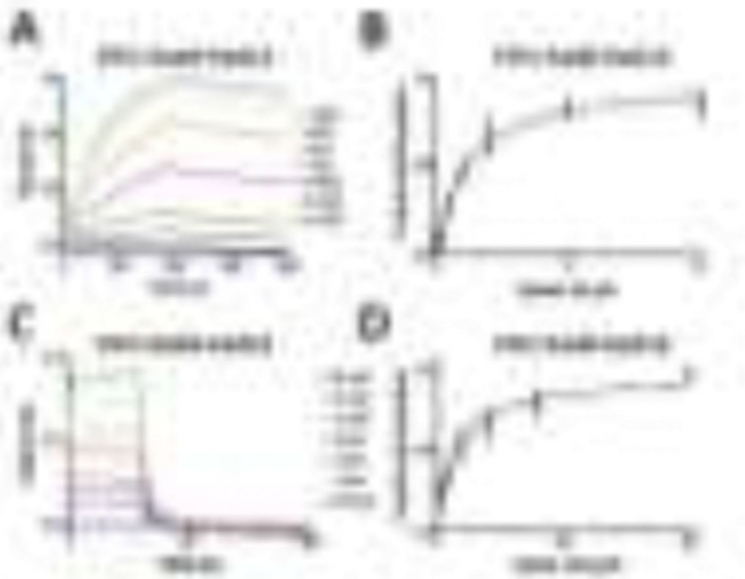

Figure 5. The PIP1 and PIP2 motifs of pol η bind Rad6-Rad18 with different affinities.

(**A**) The response units from BLI were graphed as a function of time for a fixed concentration of the PIP1 of pol η and various concentrations of Rad6-Rad18 (0.1 to 10 μM). The association phase spanned 0 to 300 s, and the dissociation phase spanned 300 to 600 s. (**B**) The equilibrium response units for each concentration of Rad6-Rad18 were expressed as fractional saturation and graphed as a function of Rad6-Rad18 concentration. The best fit of the data to the Adair equation yielded a K_d equal to 1.2 ± 0.1 μM. (**C**) The response units from BLI were graphed as a function of time for a fixed concentration of the PIP2 of pol η and various concentrations of Rad6-Rad18 (0.5 to 50 μM). The association phase spanned 0 to 35 s, and the dissociation phase spanned 35 to 100 s. (**D**) The equilibrium response units for each concentration of Rad6-Rad18 were expressed as fractional saturation and graphed as a function of Rad6-Rad18 concentration. The best fit of the data to the Adair equation yielded a K_d equal to 3.7 ± 0.5 μM.

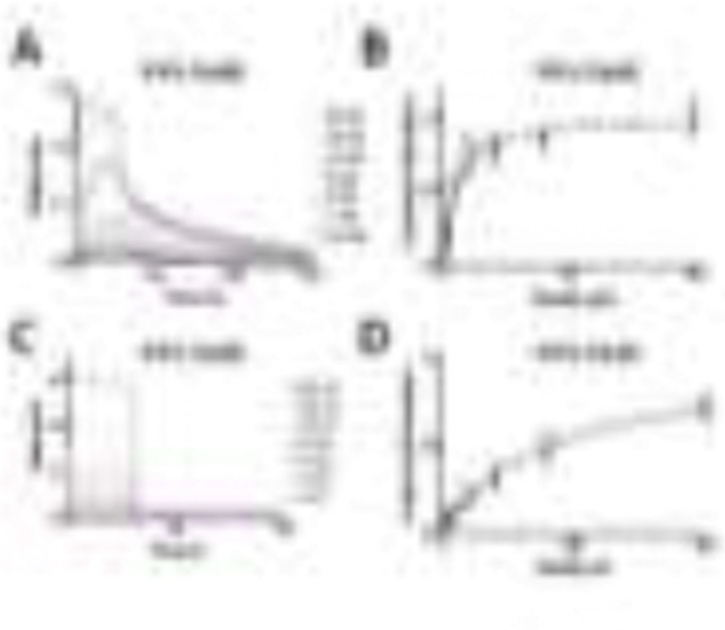

Figure 6. The PIP1 and PIP2 motifs of pol η bind Rad6 with different affinities.

(**A**) The response units from BLI were graphed as a function of time for a fixed concentration of the PIP1 of pol η and various concentrations of Rad6 (0.5 to 50 μM). The association phase spanned 0 to 60 s, and the dissociation phase spanned 60 to 300 s. (**B**) The equilibrium response units for each concentration of Rad6 were expressed as fractional saturation and graphed as a function of Rad6 concentration. The best fit of the data to the Adair equation yielded a K_d equal to 2.3 ± 0.4 μM. (**C**) The response units from BLI were graphed as a function of time for a fixed concentration of the PIP2 of pol η and various concentrations of Rad6 (5 to 500 μM). The association phase spanned 0 to 35 s, and the dissociation phase spanned 35 to 100 s. (**D**) The equilibrium response units for each concentration of Rad6 were expressed as fractional saturation and graphed as a function of Rad6 concentration. The best fit of the data to the Adair equation yielded a K_d equal to 200 ± 40 μM.

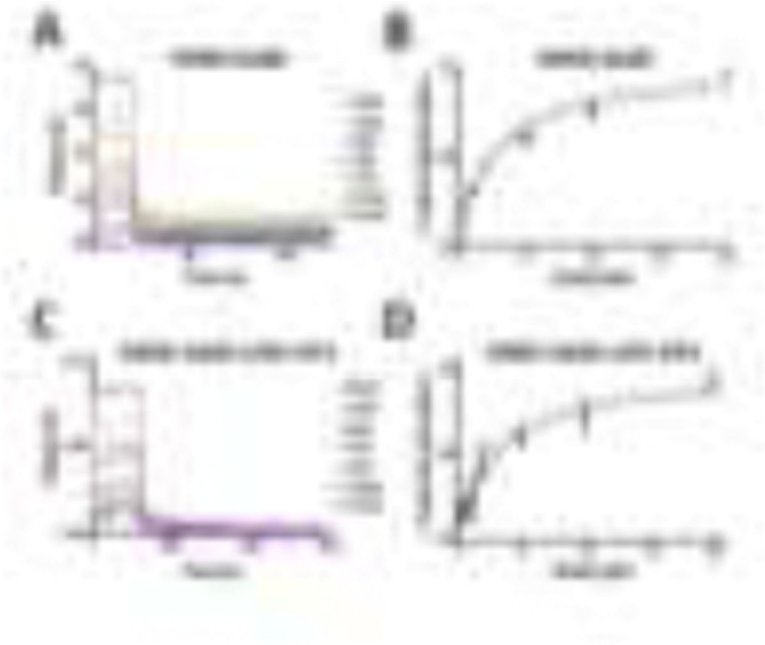

Figure 7. The PIP1 motif of pol η and the R6BD of Rad18 do not compete for binding Rad6.

(**A**) The response units from BLI were graphed as a function of time for a fixed concentration of the R6BD of Rad18 and various concentrations of Rad6 (0.2 to 20 μM) in the absence of the PIP1 motif of pol η. The association phase spanned 0 to 20 s, and the dissociation phase spanned 20 to 120 s. (**B**) The equilibrium response units for each concentration of Rad6 were expressed as fractional saturation and graphed as a function of Rad6 concentration. The best fit of the data to the Adair equation yielded a K_d equal to 2.5 ± 0.5 μM. (**C**) The response units from BLI were graphed as a function of time for a fixed concentration of the R6BD of Rad18 and various concentrations of Rad6 (0.2 to 20 μM) in the presence of the PIP1 motif of pol η (20 μM). The association phase spanned 0 to 35 s, and the dissociation phase spanned 35 to 150 s. (**D**) The equilibrium response units for each concentration of Rad6 were expressed as fractional saturation and graphed as a function of Rad6 concentration. The best fit of the data to the Adair equation yielded a K_d equal to 2.8 ± 0.4 μM.

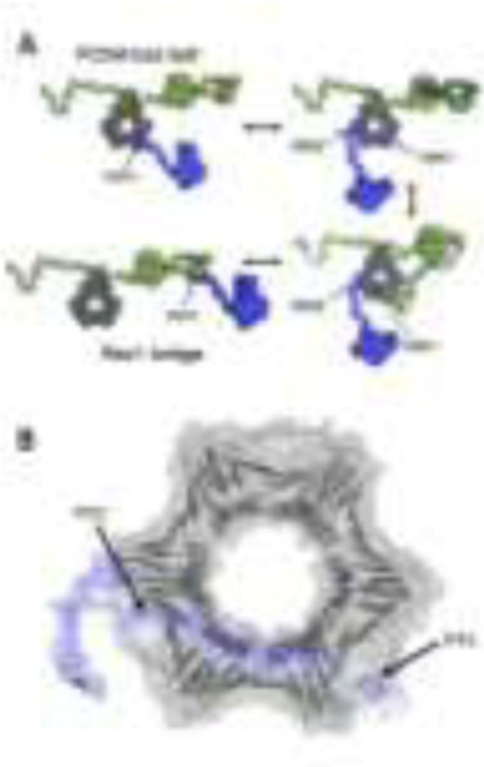

Figure 8. The PIP2 motif of pol η may mediate changes in the architecture of TLS complexes.

(**A**) When switching from the PCNA tool belt architecture to the Rev1 bridge architecture, the binding of the PIP2 motif of pol η (blue) to one subunit of PCNA (grey) would allow the transient release of the PIP1 motif of pol η from another subunit of PCNA allowing it to then bind to the CTD of Rev1 (green) without any proteins dissociating from the complex. When switching from the Rev1 bridge architecture to the PCNA tool belt architecture, the binding of the PIP2 motif of pol η to one subunit of PCNA would allow the transient release of the PIP1 motif of pol η from th CTD of Rev1 allowing it to then bind to another subunit of PCNA without any proteins dissociating from the complex. (**B**) A structural model showing a C-terminal fragment of pol η (residues 583 to 632) in blue bound to PCNA (grey). The PIP1 and PIP2 motifs of pol η can simultaneously interact with the hydrophobic pockets on the front face of two adjacent PCNA subunits.